Weak localization in high-quality two-dimensional systems

S. McPhail,[1] C. E. Yasin,[1] A. R. Hamilton,[1] M. Y. Simmons,[1] E. H. Linfield,[2] M. Pepper,[2] and D. A. Ritchie[2]
[1]*School of Physics, University of New South Wales, Sydney 2052, Australia*
[2]*Cavendish Laboratory, University of Cambridge, Cambridge CB3 0HE, United Kingdom*
(Received 5 September 2003; revised manuscript received 30 December 2003; published 14 December 2004)

We investigate five different methods of modeling the correction to the magnetoconductivity due to the weak localization effect in two-dimensional (2D) systems. The phase breaking rate is extracted using each method by fitting experimental magnetoconductivity data of high-quality 2D GaAs hole systems over the range of carrier densities and temperatures that weak localization is observed. We find that despite corrections to the magnetoconductivity differing by more than 100% between different methods valid beyond the diffusion approximation, the phase breaking rate extracted is approximately the same. We also find that if diffusive transport is incorrectly assumed in high-quality systems, then values of the phase breaking rate approximately 2.5 times too high are extracted. We demonstrate the regime in which the diffusive transport approximation holds and explain previous discrepancies in the literature where phase breaking rates much higher than expected from Fermi-liquid theory have been obtained. We find good agreement of the phase breaking rate with Fermi-liquid theory until $k_F l$ begins to approach 1.

DOI: 10.1103/PhysRevB.70.245311 PACS number(s): 73.40.Qv, 71.30.+h, 73.20.Fz

I. INTRODUCTION

Electrical measurement of the conductivity as a function of particle density, temperature, and magnetic field is a common experimental probe of the physics of two-dimensional (2D) systems of electrons and holes. At low temperature these measurements reveal information about the particle-particle interaction,[1] particle-phonon interaction,[2] and the weak localization effect.[3]

Weak localization, which is the focus of this paper, is the localization of electrons by the constructive interference of wave functions which return to the origin after propagating along time-reversed paths. The length of these paths is restricted by the phase-coherence time τ_ϕ, which determines the time scale over which quantum interference effects can operate in the system. It is well known that weak localization gives rise to a positive magnetoconductivity.[4] Increasing the magnetic field increases the conductivity by removing the time-reversal symmetry. This destroys the phase coherence of progressively shorter paths and removes the localizing effect. Analysis of this positive magnetoconductivity has been widely used to measure the phase-coherence time and probe the dephasing mechanisms in 2D systems.[5–15]

In order to reliably extract τ_ϕ from the measured data it is essential to have an accurate method for determining the effect of the weak localization on the magnetoconductivity. While a good physical understanding of the weak localization effect exists, the numerical process by which experimental data are analyzed is not so well understood. Various methods of calculating the contribution of weak localization to the magnetoconductivity $\Delta\sigma_{\rm wl}(B)$ exist in the literature.[16–20] To date these methods have not been directly compared and it is not clear whether they are equivalent or produce a different $\Delta\sigma_{\rm wl}(B)$ and hence different estimates of τ_ϕ from the same experimental data. The aim of this paper therefore is to review and compare the different methods of generating $\Delta\sigma_{\rm wl}(B)$ available and demonstrate their effect on determining τ_ϕ.

We examine five of the most commonly used methods available in the literature for calculating $\Delta\sigma_{\rm wl}(B)$, namely (i) Hikami *et al.*,[16] (ii) Kawabata,[17] (iii) Wittmann and Schmid,[18] (iv) Zduniak *et al.*,[19] and (v) Dmitriev *et al.*[20] (all of which we subsequently refer to by the first author name). Using the same data from high-quality *p*-GaAs systems we compare these methods and, in particular, choose the low carrier density regime where spin relaxation can be neglected.[21]

We show that each method predicts a markedly different correction $\Delta\sigma_{\rm wl}(B)$ to the magnetoconductivity. For high-quality systems the variation in the magnitude of the weak localization predicted by the different methods can be more than 100%. Despite this, the values of τ_ϕ extracted from the same experimental data using four of the methods agree closely and give a value close to the Fermi-liquid theory prediction for τ_ϕ. The other method, that of Hikami, is valid only in the diffusion approximation and therefore is at the limit of applicability for high-quality samples. The method of Hikami predicts a value of τ_ϕ a factor of approximately 2.5 times smaller than the other methods. This factor of approximately 3 between the value of τ_ϕ extracted using the Hikami method and the Fermi-liquid prediction has been repeatedly observed in experimental measurements of the phase breaking rate τ_ϕ^{-1} on a variety of material systems.[8,9,12–15] Our analysis of the B dependence of $\Delta\sigma_{\rm wl}$ allows us to explain the discrepancy.

The paper is laid out as follows. In Sec. II we outline the five different methods of calculating $\Delta\sigma_{\rm wl}(B)$. In Sec. III we give details of the samples and methods used to obtain and analyze the experimental data. In Sec. IV B we compare the values of $\tau_\phi(p,T)$ extracted for each method using two different samples with $r_s \sim 12$ and ~ 23 (where r_s is the ratio of the carrier's potential energy due to interactions to their kinetic energy). Following our conclusions we present, in Appendix A, typographical corrections to some of the basic references in the field (essential when calculating $\Delta\sigma_{\rm wl}$), and

finally in Appendix B we give a detailed description of the way in which we generate the quasiprobability of return of the hole to the origin, P_n. This is needed for the methods of Kawabata, Wittmann, Zduniak, and Dmitriev but has not been described in detail in the literature to date.

II. METHODS OF COMPUTING $\Delta\sigma_{\mathrm{wl}}(B)$

In this section we compare the five methods of calculating $\Delta\sigma_{\mathrm{wl}}(B)$ which are later used to extract τ_ϕ from the experimental data. These methods are as follows.

(a) Hikami (1980): An easily applicable method derived by a renormalization-group process, valid only in the diffusive transport regime.

(b) Kawabata (1984): A more complicated method derived using Green's functions. The first method developed that was valid beyond the diffusive limit.

(c) Wittmann (1987): A method derived from a different physical starting point from Kawabata, considering electron eigenstate overlap, which results in a different mathematical framework. Wittmann rescales the momentum scattering length l due to the effect of the weak localization.

(d) Zduniak (1997): An expansion of and correction to Kawabata's method which includes spin-orbit effects. Similar to Wittmann in mathematical formulation, but does not rescale the momentum scattering length due to the effect of the weak localization.

(e) Dmitriev (1997): An extension of the Kawabata method taking into account a phase-coherent nonbackscattering effect not considered by the other methods.

The first four methods have been extensively used in the literature to extract phase-coherence times from experimental data. However it is not clear from the literature which method should be applied to different experimental systems, or indeed how the methods compare. It is the intention of this paper to compare the different methods for use in extracting phase breaking rates from high-quality 2D systems. We will see that while all the methods of calculating $\Delta\sigma_{\mathrm{wl}}(B)$ yield results which are qualitatively similar, there are significant quantitative differences between them.

All five methods listed above consider isotropic large-angle scattering of the type caused by a short-ranged scattering potential. To our knowledge no analytical method exists which allows weak localization due to anisotropic small-angle scattering caused, for example, by remote ionized impurities. A recent paper[22] has numerically modeled the effect of small-angle scattering. However, as we will discuss in Sec. IV A, the values of τ_ϕ extracted from experimental data are not greatly affected by whether the analysis is performed for isotropic or anisotropic scattering.

Before discussing the methods in detail it is necessary to define our terminology. For the holes (or electrons) in a 2D system the relevant length scales when considering the weak localization effect are (i) the momentum relaxation length l, (ii) the phase relaxation length l_ϕ, and (iii) the magnetic length $l_B=\sqrt{\hbar/2eB}$ (where B is the external magnetic field perpendicular to the 2D system). From the first two length scales we find the momentum scattering time $\tau=l/v_F$ and phase relaxation time $\tau_\phi=l_\phi/v_F$ (where v_F is the Fermi velocity).

It is convenient to define two reduced parameters which are frequently referred to in the theoretical methods which follow. The first is the ratio of the elastic-scattering length to the phase relaxation length,

$$z = \tau/\tau_\phi = l/l_\phi, \tag{1}$$

which varies inversely with the magnitude of the weak localization effect. Second, the reduced magnetic field

$$b = B/B_0 = l^2/l_B^2, \tag{2}$$

where $B_0=(m^*)^2/2phe\tau^2$ and m^* is the effective mass. The reduced field is defined such that $b=1$ at $l_B=l$ or equivalently $2\pi l^2 B_0=\phi_0$ where $\phi_0=h/2e$ is the magnetic flux quantum. $z\ll 1$, $b\ll 1$ is therefore the diffusive regime, and $b\gtrsim 1$ indicates magnetically localized nondiffusive transport.

We now consider how the well-known Drude expression for the conductivity of a 2D system, $\sigma_{xx}(B)$, is modified to include the effects of weak localization. Ignoring the electron-electron interaction for the moment (it will be considered in Sec. III) we can write the conductivity as the semiclassical Drude term plus a quantum correction, $\Delta\sigma_{\mathrm{wl}}$, which accounts for phase-coherent effects:

$$\sigma_{xx}(B) = \frac{e^2}{h}\frac{k_F l}{1+\left(\frac{e\tau B}{m^*}\right)^2} + \Delta\sigma_{\mathrm{wl}}. \tag{3}$$

The perturbative expansion of $\Delta\sigma_{\mathrm{wl}}$ yields four first-order (in $1/k_F l$) terms, which may be represented by four distinct Feynman diagrams.[20] Of these, two cancel each other and need not be considered. Of the two remaining diagrams one makes a negative contribution to the conductivity and is the "conventional" weak localization pictured physically as phase-coherent backscattering of electrons. The Feynman diagram which correspond to this conventional weak localization term is sometimes known as the "maximally crossed" diagram.

The other first-order term in the expansion of $\Delta\sigma_{\mathrm{wl}}$ represents another phase-coherent contribution to the conductivity. This is positive and not included in the conventional weak localization model. It is known as nonbackscattering contribution to the weak localization. A physical picture of this positive contribution is that it represents anisotropic scattering of the carriers from the impurity potential caused by phase coherence at the origin. This should not be confused with the anisotropic small-angle scattering in samples where ionized impurities are the dominant cause of the scattering. In this case the asymmetry arises from constructive interference at the origin between paths with different numbers of scattering events. This effectively increases the chance of forward scattering at the expense of large-angle scattering events,[20] which is equivalent to increasing z and reducing the magnitude of the weak localization.

Before we can proceed we must consider whether the phase-coherence effects can be completely represented by the inclusion of $\Delta\sigma_{\mathrm{wl}}$ in Eq. (3). In 1985 it was shown by Hershfield and Ambegaokar[23] that if only the conventional weak localization correction is considered, then the momentum scattering length is reduced by a factor of $(1+z)$. A

theory which models the weak localization correction due *only* to coherent backscattering should therefore scale the momentum scattering length by this factor of $(1+z)$. As Eq. (2) shows this will reduce the value of the reduced magnetic field b by a factor of $(1+z)^2$.

Reference 23 however does not include the contribution of the phase-coherent nonbackscattering to the weak localization. If both first-order correction terms to the conductivity are taken into account, then the effect of the nonbackscattering term cancels out the effect of the coherent backscattering on the momentum scattering length.[20] This means that l and hence b do *not* need to be rescaled. Therefore Eq. (3) is correct as it is written, but implicitly assumes that both first-order contributions to $\Delta\sigma_{\mathrm{wl}}$ are included.

A. Hikami (1980)

The magnitude of the magnetoconductivity correction due to weak localization, in two dimensions, was first quantified by Hikami *et al.* via a renormalization-group method. Using the assumption that the electron transport is diffusive they produced a closed-form expression for the magnetoconductivity which may be written (in the absence of spin relaxation) as

$$\Delta\sigma_{\mathrm{wl}}(B) = \frac{-2e^2}{\pi h}\left[\Psi\left(\frac{1}{2}+\frac{1}{b}\right) - \Psi\left(\frac{1}{2}+\frac{z}{b}\right)\right], \tag{4}$$

where Ψ is the digamma function.[24] Hikami's method includes only the conventional weak localization correction to the conductivity and not the nonbackscattering correction.

Hikami's method has the dual benefits of simplicity and computational ease of use. However it is limited to the diffusive regime, and hence is valid only for low magnetic fields ($b \ll 1$) and low temperatures and/or low-quality samples where the phase-coherence length is much longer than the momentum relaxation length ($z \ll 1$). High-quality samples have large mobilities, and consequently long momentum relaxation lengths l and larger $z = l/l_\phi$. In order to study weak localization in high-quality samples it is therefore necessary to go beyond the diffusion approximation.

B. Kawabata (1984)

The method developed by Kawabata was the first to go beyond the diffusion approximation. It is, in principle, valid for all b (as are the remaining methods listed here). In fact we see later that it fails for large $b \gtrsim 20$. Kawabata employs a Green's-function method to calculate the contribution of the weak localization to the magnetoconductivity by first calculating the quasiprobability of return of an electron (or hole) to the origin after $N-1$ scattering events. The quasiprobability of return is defined in terms of P_n,

$$P_n = \frac{s}{1+z}\int_0^\infty dt L_n(t^2) e^{(-st-t^2/2)}, \tag{5}$$

where L_n is the nth Laguerre polynomial and $s = (1+z)\sqrt{2/b}$. In the absence of the nonbackscattering correction $\Sigma_{n=0}^{\infty}(P_n)^N$ may be thought of as the unnormalized probability of a particle returning to the origin after $N-1$ scattering events (note that n is an index with no physical meaning).

Once P_n is known (the process of calculating P_n is detailed in Appendix B) the weak localization correction to the magnetoconductivity can be calculated by summing over all paths with N sections ($N-1$ collisions),

$$\Delta\sigma_{\mathrm{wl}} \propto \sum_{N=3}^{\infty}\sum_{n=0}^{\infty} P_n^N. \tag{6}$$

The outer summation should not include paths with $N=1$ or 2, which do not contribute to the magnetoconductivity because they have no area. However these paths were incorrectly included in the Kawabata method.[19]

The effect of weak localization can be found by summing over all paths via

$$\Delta\sigma_{\mathrm{wl}} = -\frac{\alpha e^2}{\pi h}(F_A + F_B), \tag{7}$$

where α is a material dependent parameter which may be adjusted to account for additional scattering processes such as intervalley scattering in Si. For the p-GaAs samples studied here it is fixed at $\alpha = 1$. F_A is the coherent backscattering contribution, i.e., normal weak localization and F_B represents the contribution from the nonbackscattering mechanism. This nonbackscattering mechanism is not included in Kawabata's method, thus $F_B = 0$.

According to Kawabata's theory, F_A is given by

$$F_A = \ln\frac{1+z}{z} - 4[F_K[b(n_K+1)/4] + F_K(0)] + b\sum_{n=0}^{n_K}\frac{1}{1-P_n}, \tag{8}$$

where F_K is a function defined by Kawabata to be

$$F_K(y) = \frac{1}{4}\left[\frac{8y+(1+z)^2}{2} + \sqrt{8y+(1+z)^2} + \ln\left(\sqrt{8y+(1+z)^2}-1\right)\right]. \tag{9}$$

The first term of Eq. (8) is, neglecting the contribution of the nonbackscattering correction, the $b=0$ limit of the weak localization.[18] This is not present in Kawabata's method but it is necessary to add it as an offset so that we may later directly compare Kawabata's method with others.

The term in the summation of Eq. (8) is equivalent to the outer summation of Eq. (6) from $N=1$ to ∞. To correct for the inclusion of the $N=1,2$ terms in Eq. (8) (which cause it to diverge) Kawabata includes the diverging function F_K and finds the conductivity correction as the difference of these diverging terms. As a result of the divergences, the sum must be truncated at small n_K, where n_K is given by the closest integer to $E_F/\hbar\omega_c$. In practice, small variations in n_K caused by the variation in the particle density makes little difference to $\Delta\sigma_{\mathrm{wl}}$ and in this paper n_K was fixed at 10 for consistency with Taboryski and Lindelof.[8] Kawabata provided a recursion relation solution to Eq. (5) which allows computation of P_n up to n_K.

The Kawabata method uses the correct value of the momentum scattering length, i.e., it does not rescale it by $(1+z)$. This can be seen as a partial inclusion of the nonbackscattering correction.

C. Wittmann (1987)

Wittmann's method is essentially a version of Kawabata's that does not include the $N=1,2$ paths but does rescale the momentum scattering length by $(1+z)$. A different physical approach, considering the overlap of the electron eigenstates of the system as opposed to a Green's-function method, was used to derive the equations but the end result is similar. Thus the weak localization correction is given by Eq. (7) with

$$F_A = \frac{b}{(1+z)^2}\sum_{n=0}^{\infty}\frac{(P_n)^3}{1-P_n} \tag{10}$$

and $F_B=0$ (again the nonbackscattering is not considered). As a result of the cubic term this equation can be seen to recreate Eq. (6).

Equation (10) avoids the diverging terms of Kawabata's method but requires the summation up to large (in principle infinite) n. Large errors can result if $n<10^5$, so this method is somewhat computationally expensive. To calculate P_n to large n Wittmann *et al.* provided two new approaches to calculating P_n, which are discussed further in Appendix B.

From Eq. (10) we can see that Wittmann did include the factor of $(1+z)$ that comes from the rescaling of the momentum scattering length by the conventional weak localization. While this is perfectly consistent for a theory that only includes the conventional weak localization term, the effect of the nonbackscattering phase-coherent scattering is to cancel out the rescaling of the momentum scattering length, i.e., Wittmann (unlike Kawabata) does not include the nonbackscattering phase-coherent correction to the conductivity in any way.

D. Zduniak (1997)

Zduniak *et al.*[19] corrected Kawabata's method by removing the $N=1,2$ terms. They also expanded it by including spin-orbit effects, which become relevant when the magnetic field is smaller than $B_{so}=m^{*2}/2phe\tau_{so}^2$, where τ_{so} is the phase relaxation time due to spin-orbit effects. If we take $\tau_{so}\gg\tau_\phi$ to compare directly with the other methods, then Zduniak's method, can be simplified to

$$F_A = b\sum_{n=0}^{\infty}\frac{(P_n)^3}{1-P_n} \tag{11}$$

and $F_B=0$. Thus Zduniak's method is the same as Wittmann's except for the absence of the factor of $1/(1+z)^2$ due to the reduction of τ by the weak localization correction.

Like Kawabata's method, Zduniak partially includes the effect of nonbackscattering phase-coherent correction by leaving the value of the momentum scattering length unmodified. It is not rescaled by a factor of $(1+z)$ due the cancellation of the effects of the two first-order weak localization mechanisms. However, the nonbackscattering phase-coherent correction is not taken into account explicitly.

E. Dmitriev (1997)

The most recent method in the literature is similar to that of Kawabata, Wittmann, and Zduniak except that it also includes the contribution to the conductivity of the nonbackscattering phase-coherent correction, though not spin-relaxation effects. It is the only method which includes all first-order corrections to the magnetoconductivity.

Again we use Eq. (7) for the weak localization correction to the conductivity $\Delta\sigma_{wl}$, with F_A given by Eq. (10) and

$$F_B = -b\sum_{n=0}^{\infty}\frac{P_n((P_n^1)^2+(P_n^{-1})^2)}{2(1-P_n)}. \tag{12}$$

A new term P_n^m defined similar to P_n was introduced by Dmitriev *et al.* to account for the nonbackscattering correction:

$$P_n^m = \frac{s}{\sqrt{n+(1-m)/2}}\int_0^{\infty} dt\ t\ L^1_{n-(1+m)/2}(t^2)e^{(-st-t^2/2)}, \tag{13}$$

where L_n^1 is the first associated Laguerre polynomial and $P_0^1=0$. Note that this is a correction to the published definition of Dmitriev *et al.*[20] which is typographically incorrect[25] (other typographic errors in papers which comprise all five methods are presented in Appendix A). Details of the calculation of P_n^m are presented in Appendix B.

F. Comparison of methods

Using Eqs. (4) and (10), with F_A and F_B defined appropriately for each method, we have calculated the theoretical conductivity correction predicted by the five methods as a function of reduced magnetic field. This is shown in Figs. 1(a)–1(c) for increasing z, corresponding to increasing temperature or sample quality, respectively. All methods produce curves which show qualitatively similar positive magnetoconductivity due to the suppression of the weak localization by the magnetic field.

For small z (where $\tau_\phi\gg\tau$) and small $b\ll 1$ electron transport is diffusive. In this limit all methods appear quantitatively identical as shown in Fig. 1(a) except Dmitriev which includes the nonbackscattering correction. We also see that at low z, $\Delta\sigma_{wl}(b)$ has a strong magnetic-field dependence as electrons scatter from a large number of impurities and still return diffusively to the origin with their phases intact. The maximum number of collisions with impurities N_{max} that paths contributing to weak localization may contain is given, crudely, by $\sim 1/z$. After this their phase is randomized by inelastic processes. Therefore the conductivity correction is partly determined by long paths with large areas. Only a small magnetic field is required to destroy the phase coherence of these large area paths so the conductivity is sensitive to small changes in the magnetic field even at low b.

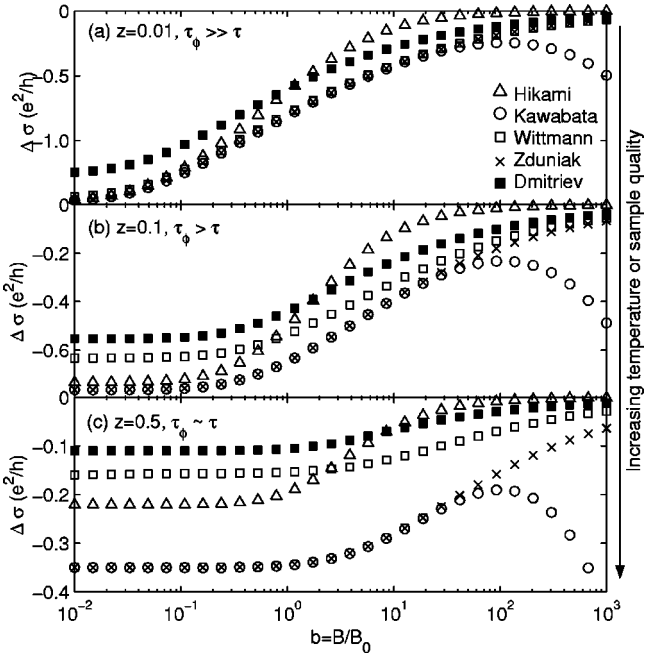

FIG. 1. (a), (b), and (c) show the conductivity correction due to the weak localization, $\Delta\sigma_{\rm wl}$, generated by the five methods with for $z=0.01$, 0.1, and 0.5, respectively. △, Hikami; ○, Kawabata; □, Wittmann; ×, Zduniak; ■, Dmitriev. Note the varying y-axis scale on each plot. The arrow on the right shows the effect of increasing temperature or, equivalently, increasing the sample quality at a fixed temperature.

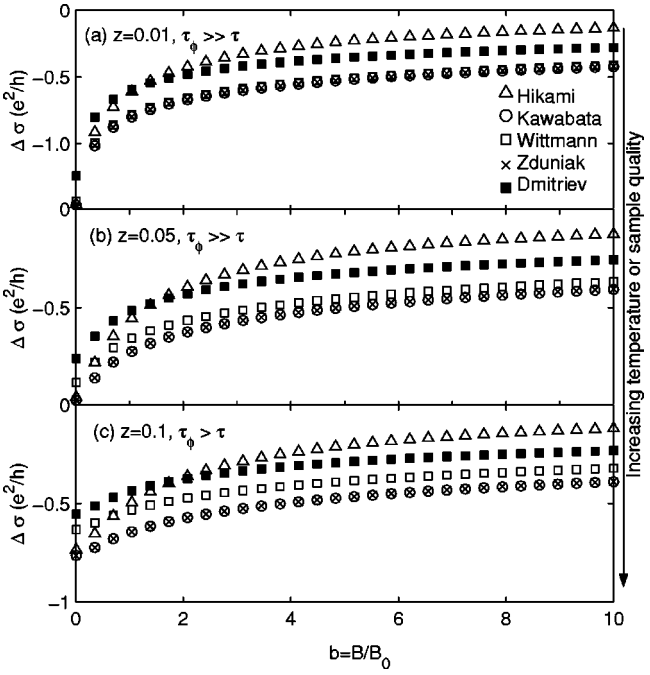

FIG. 2. In (a), (b), and (c) we have replotted the conductivity correction due to the weak localization, $\Delta\sigma_{\rm wl}$, on a linear scale. $\Delta\sigma_{\rm wl}$ is generated by each method with $z=0.01$, 0.05, and 0.1, respectively. △, Hikami; ○, Kawabata; □, Wittmann; ×, Zduniak; ■, Dmitriev. Note the different y-axis scale on each plot. The arrow on the right shows the effect of increasing temperature or, equivalently, increasing the sample quality at a fixed temperature.

As z increases to 0.1 and 0.5 in Figs. 1(b) and 1(c) we see that $\Delta\sigma_{\rm wl}(b)$ becomes quantitatively less field sensitive to changes in b up to $b\sim 1$. Here $\tau_\phi \sim \tau$ and inelastic processes destroy the phase coherence of long paths at $b\sim 0$. Therefore long paths do not contribute to the conductivity correction, so all methods give a $\Delta\sigma_{\rm wl}(b)$ which is smaller and less field sensitive at small magnetic fields than for small z.

As the magnetic field increases all methods except Kawabata predict that weak localization correction approaches zero. Increasing the magnetic field reduces the weak localization correction for two reasons, first it destroys the phase coherence of ever-shorter diffusion paths. Second, it localizes the holes (electrons), to within the magnetic length scale, reducing their ability to diffuse.

Above $b\gtrsim 20$ Kawabata's method predicts an unphysical increase in the weak localization correction, which is seen to diverge in Figs. 1(a)–1(c). This is due to the inclusion of the divergent terms discussed earlier in Sec. II B. In practice, this failure is not so important as the quantum Hall effect dominates the magnetoconductivity at these high fields and generally these data are not used for weak localization fitting.

In Fig. 2 we replot $\Delta\sigma_{\rm wl}$ for the five methods, on a linear scale, over the range of b and z that is relevant to our experimental data. It is the magnetic-field dependence of $\Delta\sigma_{\rm wl}$ in these ranges that determines the values of τ_ϕ extracted from our experimental data in Sec. IV B.

We first compare the Hikami method, which is the only method valid only in the diffusive limit, with the others. As z increases from $z\sim 0.1$ to 0.5 Hikami predicts an increasingly different dependence of $\Delta\sigma_{\rm wl}$ on b than the other methods, even for low b. Figure 2 shows that the gradient of $\Delta\sigma_{\rm wl}$ predicted by Hikami is considerably steeper across the whole range of b and z than for any of the other methods.

The Hikami method is known to be invalid at $b\sim 1$ due to the violation of the diffusion approximation by magnetic localization.[17] By comparing $\Delta\sigma_{\rm wl}$ predicted by the Hikami method with the other methods we can better quantify it's limits of validity. The Hikami method can be most directly compared with that of Zduniak and Kawabata, as neither Zduniak nor Kawabata rescale the momentum scattering length l, and include only the conventional weak localization. Deviations of the Hikami trace from that of Zduniak and Kawabata therefore shows when the Hikami method is moving outside its range of validity. From Figs. 1 and 2, and other plots at intermediate z (not shown) we can quantify the limits of validity of the Hikami method to be $z\lesssim 0.2$, $b\lesssim 0.1$.

Therefore the method of Hikami is valid for only a fraction of a typical set of temperature-dependent data. Due to the insensitivity of the magnetoconductivity to changes in the magnetic field at low b and moderate z we see that interpreting data from high-quality samples (which have large momentum scattering times and therefore large z values) requires going to magnetic fields approaching $b=1$ or more. However, for $b\gtrsim 0.1$ the diffusion model we have been considering breaks down and the method of Hikami is no longer appropriate.

We now compare three of the other methods, those of Kawabata, Wittmann, and Zduniak, which are valid beyond the diffusion approximation. We begin with Kawabata and Zduniak which we might expect to be dissimilar given the differences in Eqs. (8) and (11). However it is noteworthy that even though Kawabata's method is formally incorrect[19] and only uses values for P_n with $n \leqslant 10$, it produces for all z (as long as $b \lesssim 20$) results almost indistinguishable from that of Zduniak [which requires computation of the series in Eq. (10) up to approximately 10^5 terms]. These results suggest that in the absence of spin-orbit coupling, and below $b \sim 20$, the method of Kawabata is functionally equivalent to Zduniak while being more computationally efficient. In the remainder of this section the methods of Zduniak and Kawabata are treated identically.

For small z, Wittmann and Zduniak are almost identical as the factor $(1+z)^2$ for rescaling of the momentum scattering length is nearly negligible. As z increases Wittmann predicts a progressively smaller weak localization correction to the conductivity. However the rescaling by $(1+z)^2$ causes only a small difference in the predicted field dependence of the conductivity. As a result the field dependence $d\Delta\sigma_{\mathrm{wl}}/db$ for the Wittmann method is very similar to that of Zduniak.

The last method valid beyond the diffusion approximation is that of Dmitriev. This method shows an obvious difference from that of Zduniak for all the values of z plotted in Figs. 1(a)–1(c). Zduniak and Dmitriev use the same expressions for F_A, thus any difference between $\Delta\sigma_{\mathrm{wl}}$ in the two methods is due to the nonbackscattering correction, included as F_B in Dmitriev. Recall that the nonbackscattering effect reduces the magnitude of the weak localization, similar to increasing the momentum relaxation time of the electrons and effectively increasing $z=\tau/\tau_\phi$. The suppression of the weak localization at $b=0$ by the nonbackscattering mechanism therefore grows stronger as z increases, as can be seen in Fig. 1. At $z=0.1$ the difference in $\Delta\sigma_{\mathrm{wl}}$ caused by the inclusion of the nonbackscattering mechanism is around 30% at low b. At higher z the difference grows to a factor of 2–3 but again the field dependence $d\Delta\sigma_{\mathrm{wl}}/db$ is very similar for the two methods.

As z increases both Wittmann and Dmitirev predict a progressively smaller weak localization correction than Zduniak. While for a different reason in each case (rescaling of l and inclusion of the nonbackscattering effect, respectively), the two methods in fact predict values of $\Delta\sigma_{\mathrm{wl}}$ which are consistent to $\sim$20% over the whole range of z and b. Wittmann predicts approximately the same field sensitivity for $\Delta\sigma_{\mathrm{wl}}$ as Dmitriev.

In summary, $\Delta\sigma_{\mathrm{wl}}$ predicted by Hikami is considerably more field sensitive than for methods valid beyond the diffusion approximation and these latter methods produce very similar magnetoconductivity corrections, except for a field-independent offset. We now move on to consider how these methods are used to interpret experimental magnetoconductivity data.

III. EXPERIMENTAL METHOD

We measured the low-temperature magnetoconductivity of two high-quality 2D hole systems. The samples A1433/37 and T402/5 are gated, modulation doped GaAs-AlGaAs heterostructures grown by molecular-beam epitaxy on (311)A substrates[26,27] patterned into Hall bar geometries. We use standard four terminal low-frequency lock-in measurement techniques, with measurement currents below 1.5 nA to minimize sample heating effects.

The carrier density of sample A1433/37 was measured to be $p=2.4\times10^{11}$ cm^{-2} and the mobility $\mu=2\times10^5$ cm^2 V^{-1} s^{-1} at zero gate bias. Sample T402/5 was made from an extremely high-quality heterostructure, with a much higher mobility of $\mu=8.3\times10^5$ cm^2 V^{-1} s^{-1} at $p=7.7\times10^{10}$ cm^{-2} (zero bias) and a peak mobility in excess of 1.2×10^6 cm^2 V^{-1} s^{-1}. In both samples Shubikov de Haas measurements show that only the heavy-hole subband is occupied, which removes any possible dephasing from intersubband interactions.[28] While p-GaAs systems can show magnetoresistance effects due to spin-orbit coupling these only occur at high carrier density.[21] At the low densities studied here spin-orbit effects are not important and hence are not included in our analysis.

The inversion asymmetric potential of the 2D well that the holes reside in is known to split the degeneracy of the light-heavy holes leading to the formation of two carrier species with masses of m_-^* in the range $(0.15-0.23)m_e$ (Refs. 29 and 30) and $m_+^* \sim 0.38m_e$.[31] In view of this we take an average value of $m^*=0.3m_e$.[32]

For each sample we measured ρ_{xx} and ρ_{xy} at low B for a variety of temperatures and densities. A typical example for sample A1433/37 at a density of 4.5×10^{10} cm^{-2} is shown in Fig. 3(a). Matrix inversion was performed on the ρ_{xx} and ρ_{xy} traces to produce the conductivity σ_{xx} and σ_{xy} as a function of magnetic field,

$$\sigma_{xx}(B)=\frac{\rho_{xx}}{\rho_{xx}^2+\rho_{xy}^2},\quad \sigma_{xy}(B)=\frac{\rho_{xy}}{\rho_{xx}^2+\rho_{xy}^2}, \tag{14}$$

as shown in Fig. 3(b).

For high mobility samples ρ_{xx} and ρ_{xy} are of comparable magnitude (as $\rho_{xx}\sim\rho_{xy}/B\mu$). Therefore there is a significant negative parabolic magnetoconductivity in $\sigma_{xx}(B)$ arising from the field dependence of ρ_{xy}. The dashed line in Fig. 3(b) shows the negative magnetoconductivity in the absence of weak localization. The positive magnetoconductivity due to the weak localization is superimposed onto this negative magnetoconductivity background. Figure 3(c) shows the positive magnetoconductivity due to the weak localization effect alone, and is the difference between the measured σ_{xx} trace and the dashed line in Fig. 3(b).

At small magnetic fields where the quantum Hall effect is negligible ($B \lesssim 0.25$ T in these samples) we use the semiclassical Drude formalism to describe the transport in our 2D samples. The negative magnetoconductivity arises from localization of the electrons in cyclotron orbits. We include two quantum correction terms $\Delta\sigma_{\mathrm{wl}}$ due to the weak localization (discussed in Sec. II) and $\Delta\sigma_{\mathrm{hh}}$, due to the hole-hole interaction. The conductivity is then

$$\sigma_{xx}(B)=\frac{\sigma_0}{1+\left(\frac{e\tau B}{m^*}\right)^2}+\Delta\sigma_{\mathrm{wl}}(B,z)+\Delta\sigma_{\mathrm{hh}}, \tag{15}$$

where $\sigma_0=pe^2\tau/m^*=(e^2/h)k_Fl$.

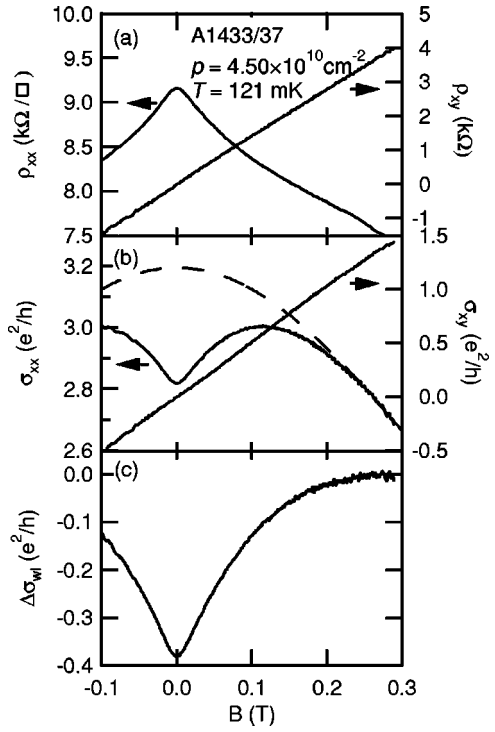

FIG. 3. (a) Typical low field ρ_{xx} and ρ_{xy} data, (b) the derived σ_{xx} and the sum of the Drude and hole-hole interaction terms (dashed line), and (c) the difference of the σ_{xx} data and the fitted Drude and hole-hole terms. These data come from sample A1433/37 with $p = 4.50\times10^{10}$ cm^{-2}.

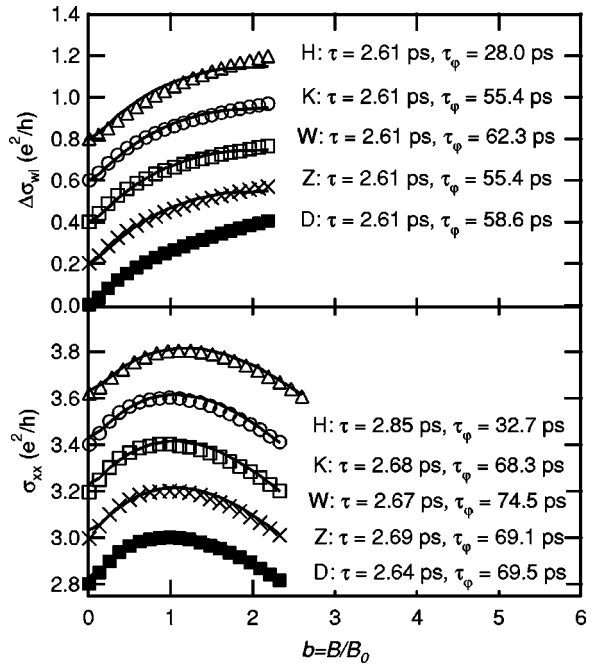

FIG. 4. (a) Comparison of fitted points (symbols) and experimental data for each of the five methods using the two-stage procedure fit. The experimental data (solid line) come from A1433/37 with $p = 4.50\times10^{10}$ cm^{-2}; symbols give best fit according to method; △: Hikami; ○, Kawabata; □, Wittmann; ×, Zduniak; ■, Dmitriev. Each method is offset with associated experimental data by $0.2e^2/h$ for clarity. (b) Simultaneous three-parameter fit results, again from sample A1433/37 with $p = 4.50\times10^{10}$ cm^{-2}, each method is offset by $0.2e^2/h$ for clarity. Note that the experimental data appears different in each fit in (b) because the scaling of the reduced magnetic field depends on τ.

This approach is strictly valid only when the holes can be treated as particlelike wave packets on the scale of the impurity separation, i.e., $k_F l \gg 1$ (which is equivalent to $\sigma_0 \gg e^2/h$). Equation (15) also assumes that the quantum corrections $\Delta\sigma_{\rm hh}$ and $\Delta\sigma_{\rm wl}$ are small compared to the Drude term. At the low carrier densities we are using this theoretical framework is near the limits of its validity but is considerably more appropriate than models of hopping conduction, which are only valid when $\sigma_0 \ll e^2/h$.

We use Eq. (15) to fit our magnetoconductivity traces. It contains three fitting parameters: τ (the momentum relaxation time), z (given by τ/τ_ϕ), and $\Delta\sigma_{\rm hh}$ (the contribution to the magnetoconductivity from the hole-hole interaction). It is known[33] that the magnetic-field dependence of the conductivity due to hole-hole interaction, $\Delta\sigma_{\rm hh}$, is negligible for $g\mu_B B \ll k_B T$. For our devices $g\mu_B B \lesssim k_B T$ even at our lowest temperatures and highest fields. This means that the magnetic-field dependence of the hole-hole contribution to σ is weak. Including the magnetic-field dependence of the singlet channel interaction term[33] changes the extracted values of τ_ϕ by $\approx$5%. Given the uncertainty about the field dependence of the triplet term, we have neglected the hole-hole interaction term and treated $\Delta\sigma_{\rm hh}$ as a constant.

For the data analyzed here the perpendicular magnetic field need to spin polarize the 2D system $\sim E_F/g\mu_B$ is several tesla. The fields used are $\lesssim$0.25T which will not greatly affect the ratio of the spin populations and hence the hole-hole interaction. Therefore the magnitude of the hole-hole correction to the magnetoconductivity is treated as field independent.

Two things are necessary to extract τ, z, and $\Delta\sigma_{\rm hh}$ from the experimental data by fitting with Eq. (15). First, a method must be available to calculate the contribution to the conductivity as a function of b and z — this is one of the five methods described in Sec. II. Second, a procedure is needed to fit the weak localization contribution to the magnetoconductivity data and estimate the value of τ_ϕ.

The analysis of high-quality samples (where $\rho_{xx} \sim \rho_{xy}$) is complicated by the overlap of the parabolic negative magnetoconductivity and the positive magnetoconductivity due to the weak localization. We detail two possible procedures to take account of this, so that we can fit the weak localization and hence extract τ_ϕ. The first has been used previously in the literature and the second we have developed and used here. The two procedures produce approximately consistent results.

In the first fitting procedure,[11] shown in Fig. 4(a), the Drude and hole-hole interaction terms are fitted to the highest magnetic-field data available before the quantum Hall effect becomes significant, $B \gtrsim 0.25$ T. The first fit of the high-field data fixes τ and allows the Drude and hole-hole interaction contributions to the low-field magnetoconductivity [shown in Fig. 3(b) as the dashed line] to be determined. The contribution of the weak localization to the magnetoconductivity is then determined by subtracting the dashed line

from the experimentally measured σ_{xx} to give the data shown in Fig. 3(c).

We can now extract the value of τ_ϕ by fitting $\Delta\sigma_{\rm wl}$ predicted by Eq. (4) (the Hikami method) or Eq. (7) using the appropriate expressions for F_A and F_B (the Kawabata, Wittmann, Zduniak, or Dmitriev methods) as demonstrated in Fig. 4(a). In each case we have fitted over the whole range of available data and extracted the values for τ and τ_ϕ. For this procedure the value of τ extracted is independent of the method of generating $\Delta\sigma_{\rm wl}$. We see that the four methods valid beyond the diffusion approximation produce similar values of τ_ϕ while the method of Hikami gives a significantly smaller one. This will be discussed in detail in the following section.

Close examination of the fits in Fig. 4(a) shows that the residuals[34] are correlated to some extent, i.e., the fit deviates from the experimental data through more than statistical error. This is not surprising as we have not included contributions to the magnetoconductivity that may arise from the field dependence of the hole-hole interactions,[35] spin relaxation,[7,19] and antilocalization due to subband filling or interface roughness.[28] In addition, as mentioned earlier, Eq. (15) strictly applies only for $k_F l \gg 1$. Nevertheless the experimental data can be reasonably well replicated by varying the fitting parameters τ, τ, and $\Delta\sigma_{\rm hh}$.

In the *second* fitting procedure we use a *simultaneous* three-parameter fit of Eq. (15) without separating the weak localization contributions from the Drude magnetoconductivity. The parameter τ is used to generate the Drude term and the parameter z and the magnetic field b are the inputs to the five methods of generating $\Delta\sigma_{\rm wl}$. Typical three-parameter fits are given in Fig. 4(b). The raw data in each case are identical but the x-axis scaling differs slightly due to the different values of τ. These fits show the same small nonstatistical deviations from the data as Fig. 4(a). Again we see that the four methods valid beyond the diffusion approximation produce similar values of τ_ϕ while Hikami produces a significantly lower value.

The simultaneous three-parameter fitting procedure is faster, simpler, and less subjective than the two-stage procedure as no decision need be taken as to the fitting range of the first stage. However the function which is being fitted to the σ_{xx} data of Fig. 4(b) is the sum of the three terms in Eq. (15) rather than only the $\Delta\sigma_{\rm wl}$ term to the data of Fig. 3(c) and as such it is not as intuitively simple to interpret.

In both procedures the fitting for each method shown in Figs. 4(a) and 4(b) is done over the full range of data. It is known that the methods of Kawabata, Wittmann, Zduniak, and Dmitriev are valid over the full range of data. In contrast the method of Hikami is not theoretically valid over the full range of data. However we have found that fitting Hikami over all values of b produces values of τ_ϕ within $\sim$10% of those found by fitting only the $b<0.5$ data,[10] i.e., limiting the fit with Hikami to $b<0.5$ has no significant effect on the resulting value of τ_ϕ extracted.

We can see that in both fitting procedures the method of Hikami gives at least as good a fit as the other methods even though it is invalid over most of the range of b. These results emphasize that without a detailed analysis of the validity of each of the methods it is impossible to judge — on the basis of the fit alone — whether the method is valid under the conditions of use and therefore whether the extracted parameters may be trusted.

Each of the two fitting procedures produce similar values for τ_ϕ^{-1}, within 15%. For each of the two fitting procedures Hikami produces a value of τ_ϕ significantly lower than the other methods (for which τ_ϕ is approximately the same). There is however a small difference between the procedures, for the methods valid beyond the diffusion approximation the two-stage fit gives results for τ_ϕ that are consistently lower than those of the three-parameter fit results.

There are two main reasons for the differences between the two different fitting procedures. First, the two-stage procedure explicitly assumes that there is no effect due to the weak localization correction at high field ($b \gtrsim 1$ in this case). Although this is not true (Fig. 1 shows that $\Delta\sigma_{\rm wl}$ is still significant at $b\sim1$) this produces only a small change in τ. This can be seen by comparing the values derived for τ using the two fitting procedures shown in Fig. 4, which agree to within $\sim$10%. Second, the two-stage procedure fixes the theoretical value of $\sigma_{xx}(B=0)$ to be identical to the experimental value of $\sigma_{xx}(B=0)$ whereas the three-parameter fit allows the curves to "float" over each other until the best fit is found. This reduces the parameter space available to the two-stage fit somewhat and also makes it vulnerable to systematic errors that exist only at very small fields, for example, spin-relaxation-induced antilocalization[7,19] or subband/interface roughness effects.[28] These systematic effects will also affect the parameters induced from the three-parameter fit. However, the quality of the three-parameter fit will suffer less because this procedure does not force the fit to be the same as the experimental data at the point which the systematic errors are at their largest. For this reason we fit all the remaining data with the three-parameter fitting procedure.

Having fit the full range of data we must first consider another complication before we determine the temperature dependence of τ_ϕ. We must ensure that the temperature of the holes is well known — it is not enough to simply monitor the lattice temperature of the heterostructure and assume that the two are the same. Unavoidable experimental limitations (the lack of phonons to thermalize the holes at low temperatures) frequently limit the temperature of the 2D hole system, as distinct from the temperature of the crystal lattice, to $\gtrsim$100 mK.[36] This has the effect that any temperature-dependent quantity such as the phase breaking rate will appear to saturate as the measured temperature approaches zero. We have therefore determined the hole temperature independent of the lattice temperature by using the 2D hole system as its own thermometer. This was achieved by measuring the resistivity at the $\nu=2$ Shubnikov de Haas minima, and fitting it to an exponential activation function, as shown in Fig. 5(a). The plotted points deviate from the expected activation behavior exponential at low temperature when the hole temperature deviates from the lattice temperature. The relationship of the lattice temperature and hole temperature determined in this way is shown in Fig. 5(b). For temperatures above 200 mK, the two are always in good agreement. However significant deviations are found at lower temperatures. Therefore τ_ϕ is analyzed as a function of the temperature of the 2D hole system itself, $T_{\rm hole}$, determined from the Shubikov de Haas oscillations.

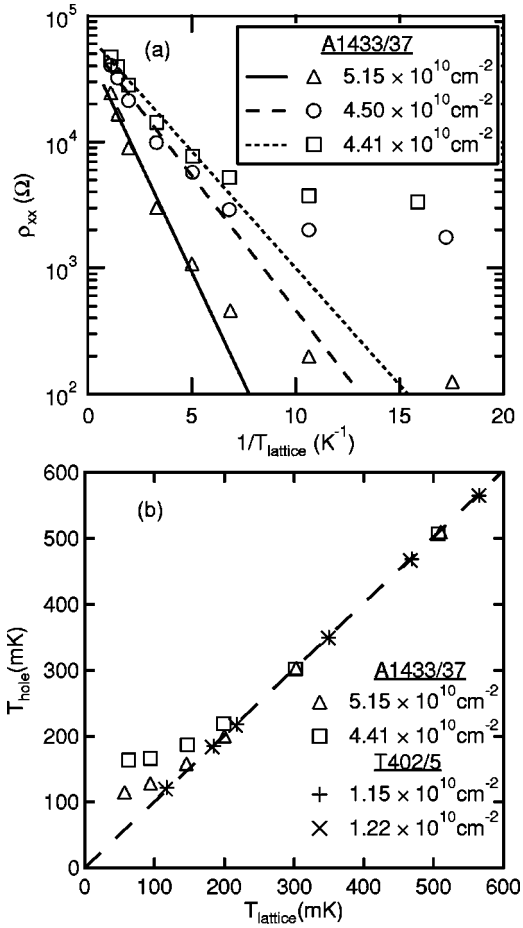

FIG. 5. (a) Activation plots for three different sample densities for A1433/37. The lines are least-squares fits to the five highest-temperature points. (b) T_{hole} vs T_{lattice} plots for each sample at the extremes of the density range studied.

To summarize, we have found a preferred fitting procedure [distinct from the five different methods of generating $\Delta\sigma_{\mathrm{wl}}(b)$ described in the preceding section], which shows that significantly different values of τ_ϕ may be extracted from the same conductivity data depending whether Hikami's method or one valid beyond the diffusion approximation is used. Having also used the correct hole (not lattice) temperature, we are in a position to analyze data for both samples at different p and T to investigate the temperature and density dependence of τ_ϕ.

IV. RESULTS AND DISCUSSION

A. Extracting τ_ϕ from experimental data

To determine the effect of using the five different methods of generating $\Delta\sigma_{\mathrm{wl}}$ on the derived value of τ_ϕ, we analyze the magnetoconductivity data for both samples using each method. We also compare the values of τ_ϕ that we extract with others in the literature for p-GaAs systems.

First, it is important that the density dependence of σ is understood. As the carrier density increases the weak localization correction becomes harder to observe in the Drude magnetoconductivity, because the Drude contribution becomes larger and more strongly peaked as p increases. The density dependence of the Drude term can be understood from Eq. (15) noting that τ increases with increasing p. Thus the small weak localization signal is lost in the rapidly increasing conductivity. In contrast at lower densities the weak localization description breaks down as the two-dimensional hole system breaks up into isolated "islands" and charge becomes strongly localized, transport taking place by variable range hopping.[4] Therefore there is only a limited range over which weak localization is clearly observable. It is this "window" that forces us to work close to the limit of $k_F l \sim 1$, where the Drude picture becomes invalid.

Figure 6(a)–6(c) shows magnetoconductivity data for A1433/37 at three different hole densities, $p = 4.41 \times 10^{10}$, 4.50×10^{10}, and 5.15×10^{10} cm^{-2}. Data are presented at the lowest attainable hole temperature and for the full range of density over which weak localization is observed in these samples. Over this density range the device has a conductivity of $>2.5\ e^2/h$ which just satisfies the condition for validity of Eq. (15) and Fermi-liquid theory, $\sigma \gg e^2/h$. Each trace shows both the positive magnetoconductivity at low magnetic fields due to the weak localization and the negative magnetoconductivity at higher fields caused by magnetic localization. The magnitude of the weak localization correction at zero magnetic field, $\Delta\sigma_{\mathrm{wl}}(B=0)$, is approximately constant over the full range of density. This can be seen by comparing the absolute magnitude of the positive magnetoconductivity in Figs. 6(a)–6(c). There is no sign that the magnitude is strongly suppressed by the increasing carrier density, agreeing with Refs. 9 and 36 though in contrast to Ref. 37.

The magnetoconductivity data were fitted using the three-parameter fit procedure described in Sec. III and each of the five methods of generating $\Delta\sigma_{xx}$ described in Sec. II. The values of τ_ϕ produced were inverted and plotted in Figs. 6(d)–6(f). We note that the values extracted for the four methods valid beyond the diffusion approximation are the same within $\lesssim 10\%$ with the Hikami model predictions being significantly greater. In addition, we plot as solid and dashed lines the predictions of Fermi-liquid theory for τ_ϕ^{-1} in the limit $k_B T\tau/\hbar \ll 1$ most appropriate to our samples (discussed below).

At first glance there are two puzzling things about the values of τ_ϕ extracted by the five methods. The first is that the values of τ_ϕ^{-1} extracted using Hikami are dramatically significantly larger than those from the four methods valid beyond the diffusion approximation, though $\Delta\sigma_{\mathrm{wl}}$ predicted by the Hikami method is qualitatively similar to the others. The second is the surprising similarity of the predictions of the four methods valid beyond the diffusion approximation, given the large differences in $\Delta\sigma_{\mathrm{wl}}(B)$ that each predicts. Over the ranges of b and z that the data span ($0.01 \lesssim b \lesssim 1.2$ and $0.02 \lesssim z \lesssim 0.1$) $\Delta\sigma_{\mathrm{wl}}(B)$ varies by up to $\sim 200\%$ between the four methods while τ_ϕ only varies by $\lesssim 10\%$.

We can resolve both of these puzzling observations about the τ_ϕ results by considering the fitting process and the shape of the curves plotted in Fig. 2. In the simultaneous three-parameter fit the presence of the hole-hole interaction term is identical in effect to a magnetic-field-independent offset to the magnitude of $\Delta\sigma_{\mathrm{wl}}(b)$. This means that a fit of two methods (Dmitriev and Kawabata, for example) which predict a

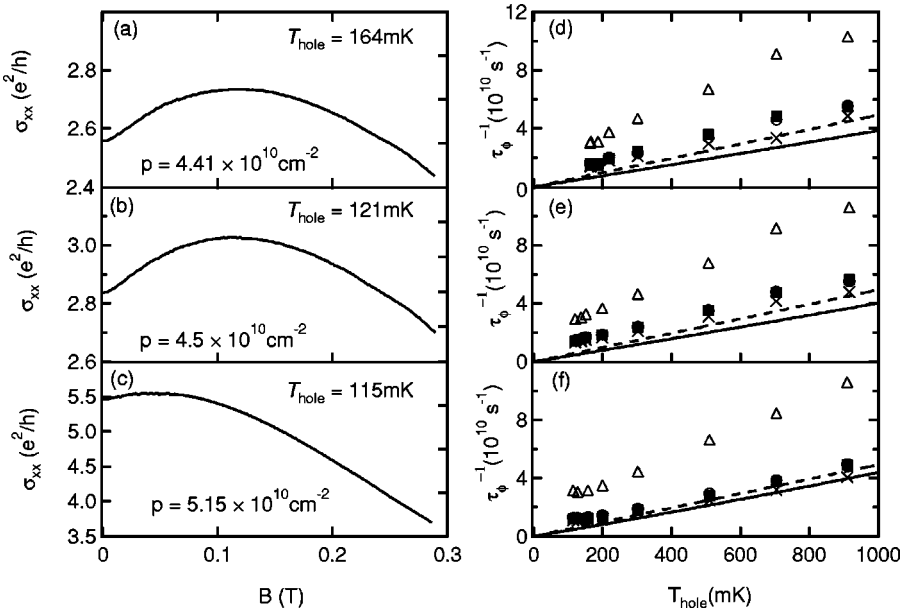

FIG. 6. (a)–(c) Magnetoconductivity data for sample *A*1433/37 at the density and temperatures indicated, and (d)–(f) τ_ϕ^{-1} computed by each method of generating $\triangle\sigma_{wl}$. Δ, Hikami; ○, Kawabata; □, Wittmann; ×, Zuduniak; and ■, Dmitriev. The solid and dashed lines show predictions of Fermi-liquid theory according to Eq. (16) with $F_0^\sigma = -0.3$ and 0, respectively.

difference in $\Delta\sigma_{wl}(b)$ which is only a field-independent constant will produce exactly the same value of τ_ϕ but a different value of $\Delta\sigma_{hh}$. A similar argument applies to the two-stage fitting procedure described in Sec. III in which the magnitude of the weak localization is offset explicitly to zero. This occurs when it is assumed that the theoretical and experimental values of $\Delta\sigma_{wl}(b)$ are identical at $b=0$ and the remainder of the fitting procedure done relative to the value of $\Delta\sigma_{wl}(b=0)$. This explains the similarity of the values of τ_ϕ given in Fig. 4 for the two fitting methods.

Therefore, using either fitting procedure, the magnitude of the conductivity correction is much less important than the predicted field dependence $d\Delta\sigma_{wl}(b)/db$, over the range of b and z used for data fitting. As Fig. 2 shows $d\Delta\sigma_{wl}(b)/db$ is almost the same in each of the four methods valid beyond the diffusion approximation, but much larger in the Hikami method. We can now understand why each of the methods valid beyond the diffusion approximation give such a similar estimate of τ_ϕ: apart from the field-independent offset the magnetoconductivity correction for each method is very similar in shape. It is also clear why the method of Hikami produces such a different prediction of τ_ϕ than the other methods — the field dependence of its predicted $\Delta\sigma_{wl}(b)$ is much steeper. Therefore to fit the same experimental data (as is shown in Fig. 4) it returns a much smaller value of τ_ϕ. We can sum up both these effects by observing that for extracting τ_ϕ it is the gradient of the magnetoconductivity correction plotted in Fig. 2 that is important, not its magnitude.

It is interesting to compare our analysis of our experimental data with recent numerical simulations of the magnetoconductivity beyond the diffusion approximation. At first glance our results are different from another previously reported study by Minkov *et al.*[35] which found a reasonable agreement between the methods of Hikami and Wittmann. We note that there is a critical difference between our method and that of Minkov *et al.* In our fits the parameter α, defined in Eq. (7), is fixed at the theoretical value of 1. Minkov *et al.* use as a fitting parameter in the Hikami method and find values of $\alpha \sim 0.5$. The values extracted for α and τ_ϕ are not independent, so if Minkov *et al.* had fixed $\alpha=1$, then values of τ_ϕ in close agreement with ours would have been extracted. Thus the numerical simulations and our analysis are in fact consistent.

In addition, there has been recent interest in the difference between isotropic (from short-range potentials) scattering and anisotropic (from wide potentials) scattering.[22] Most theoretical work has concentrated on isotropic scattering, which will occur in Si metal-oxide-semiconductor field-effect transistor, whereas in high-quality modulation doped GaAs systems the scattering may be anisotropic. However, both produce $\Delta\sigma_{wl}(B)$ traces which have similar values of $d\Delta\sigma_{wl}/db$ and hence by a similar argument to that above (for the different fitting methods valid beyond the diffusion approximation) can be expected to produce similar values of τ_ϕ. Therefore these methods can be used to extract τ_ϕ even from samples in which the scattering is anisotropic although values of $\Delta\sigma_{hh}$ will be less reliable.

B. Analysis of the phase breaking rate in *p*-GaAs

Comparable *p*-GaAs devices to those studied here have been fitted previously using the method of Hikami.[10,13] Both studies find values of τ_ϕ three to five times smaller than those predicted from Fermi-liquid theory. Phase breaking rates τ_ϕ^{-1} have also been extracted and compared to theoretical values in other material systems, for example, *p*-SiGe,[9,15] and Si.[12] In all these cases where the method of Hikami was used to fit the data, the value of τ_ϕ extracted was found to differ by the factor of 3–5 from the theoretical value. We explain this discrepancy as being due to the use of the Hikami method in a range beyond its validity in these high-quality samples, where the diffusion approximation can no longer be relied upon. To our knowledge the five various fitting methods have not been directly compared so this dependence on the fitting method has not previously come to light.

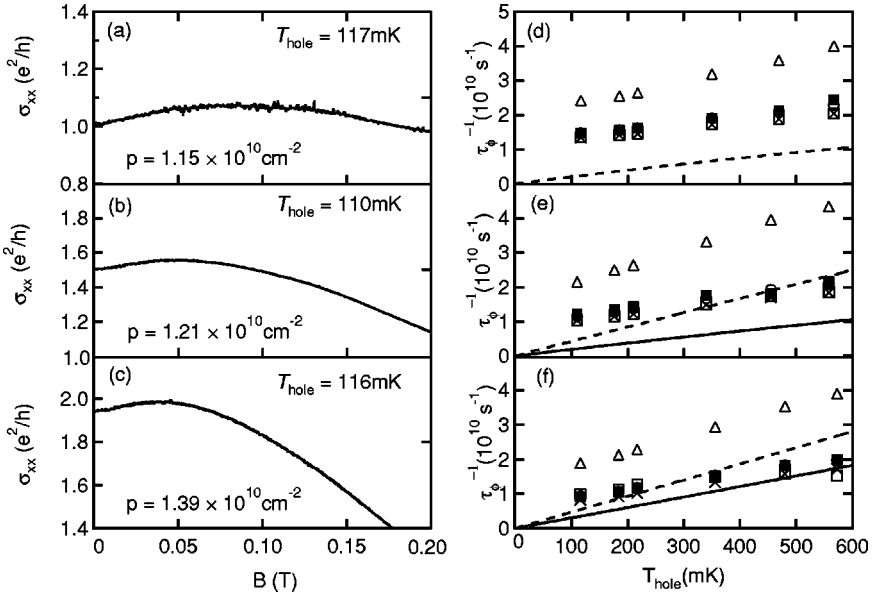

FIG. 7. (a)–(c) Magnetoconductivity data for sample *T*402/5 at the density and temperatures indicated and (d)–(f) τ_ϕ^{-1} computed each method of generating $\triangle\sigma_{\rm wl}$. Δ, Hikami; ○, Kawabata; □, Wittmann; ×, Zuduniak; and ■, Dmitriev. The solid and dashed lines show predictions of Fermi-liquid theory according to Eq. (16) with $F_0^\sigma=-0.3$ and 0, respectively. For (a) this produces a negative prediction of τ_ϕ in the $F_0^\phi=-0.3$ case as discussed in the text.

It is interesting to note that the magnitude of $\Delta\sigma_{\rm wl}(B)$ is important for extracting $\Delta\sigma_{\rm hh}$, and while the size of the hole-hole correction is not explored in this paper the choice of methods valid beyond the diffusion approximation produce significant differences in this parameter.

We now use the values of τ_ϕ extracted by the Dmitriev method to probe the nature of the hole state in our high-quality samples. At high carrier densities 2D systems are known to be a Fermi liquid but as the density is lowered the ratio of the interaction energy to the kinetic energy, r_s, becomes large and the nature of the 2D system is uncertain. Recently it has been suggested that Fermi-liquid theory, which does not take into account strong particle-particle interactions, can be modified to account for them.[38] We therefore compare the temperature dependence of the dephasing rate τ_ϕ^{-1} to the predictions of this modified version of Fermi-liquid theory.

Fermi-liquid theory predicts dephasing due to inelastic particle-particle interactions with a characteristic rate (i.e., τ_ϕ^{-1}) that has both a linear and a quadratic temperature-dependent component. These arise from the Coulomb interaction of the particles with and without the mediation of an impurity, respectively.[39] The prefactors of the T and T^2 terms depend on the whether the Fermi surface is smeared by temperature or disorder: they are only well defined in the limits $k_BT\tau/\hbar\ll1$ and $k_BT\tau/\hbar\gg1$ and in either case vary slightly between different theoretical treatments.[38]

For the traces presented in Fig. 6, sample A1433/37, we have $0.04<k_BT\tau/\hbar<0.41$. For all carrier densities the temperature dependence of τ_ϕ appears linear (for each method of generating $\Delta\sigma_{\rm wl}$) with little sign of a T^2 contribution, thereby justifying our choice of the $k_BT\tau/\hbar\ll1$ limit. While the values of τ_ϕ^{-1} extracted from the fits are proportional to m^*, the effective mass of the holes in GaAs, this does not affect the linearity of the data. The temperature dependence of the phase breaking rate predicted by Fermi-liquid theory including the effects of interactions is given by[38]

$$\tau_\phi^{-1}=\left[1+\frac{3(F_0^\sigma)^2}{(1+F_0^\sigma)(2+F_0^\sigma)}\right]\frac{k_BT}{\hbar}\frac{e^2}{h\sigma_0}\ln\left[\frac{h\sigma_0}{e^2}(1+F_0^\sigma)\right]+\frac{\pi}{4}\left[1+\frac{3(F_0^\sigma)^2}{(1+F_0^\sigma)^2}\right]\frac{(k_BT)^2}{\hbar E_F}\ln\left[\frac{h\sigma_0}{2e^2}\right],\tag{16}$$

where $\sigma_0=pe\mu$ is the Drude conductivity and F_0^σ is the Fermi-liquid constant, a measure of the strength of the hole-hole interactions. For the noninteracting limit ($F_0^\sigma=0$) Eq. (16) reduces to that given in Refs. 39 and 40.

We extract a value of $F_0^\sigma\sim-0.3$ for both our devices using the method of Ref. 41. We find that the inclusion of F_0^σ makes only a modest difference of ~20% to the predicted phase breaking rate [plotted in Figs. 6(d)–6(f) as the solid and dashed lines] at all carrier densities.

Figs. 6(d)–6(f) show that τ_ϕ^{-1} decreases with increasing carrier density. This behavior is in qualitative agreement with Fermi-liquid theory, which predicts less hole-hole scattering with increasing hole density. While it might be intuitively thought that a higher hole density would lead to more hole-hole scattering in fact the increase in hole screening reduces the importance of the particle-particle interactions.

The temperature dependence of the phase breaking rate derived from the Dmitriev method agrees reasonably well with the prediction of Fermi-liquid theory in the $k_BT\tau/\hbar\ll1$ limit, as Figs. 6(d)–6(f) show. This suggests that Fermi-liquid theory, modified to account for particle-particle interactions[38] provides an accurate, quantitatively predictive theory of the nature of the 2D electronic system at $r_s\sim12$.

We also performed magnetoconductivity measurements on the ultrahigh-quality sample T402/5, where $r_s\sim23$, over the complete range of densities at which weak localization can be clearly observed. We used the same three-parameter fitting procedure to extract values of τ_ϕ in order to investi-

gate the nature of the hole system at this high value of r_s.

The raw magnetoconductivity data of the ultrahigh-quality sample T402/5 is plotted in Figs. 7(a)–7(c). It shows weak localization similar to that of A1433/37 but because T402/5 is of higher quality it has a smaller weak localization correction for a similar temperature. However the magnitude of the weak localization effect is again approximately constant over the range of density studied, showing no sign of sudden disappearance as the carrier density in increased.

Values of τ_ϕ^{-1} extracted are plotted in Figs. 7(d)–7(f) at three densities which again span the range of clearly observable weak localization. For T402/5 the conductivity is necessarily closer to the limit of $\sigma_0 = e^2/h$ than A1433/37 because of the higher quality of the sample. We see that the phase breaking rates estimated using the five methods of generating $\Delta\sigma_{\rm wl}$ are again approximately linear for each method as in sample A1433/37. However the magnitude of τ_ϕ^{-1} and it's sensitivity to the temperature are both lower in T402/5. This may be understood from Eq. (16) noting that this close to $\sigma_0 = e^2/h$ the logarithmic term dominates the linear temperature dependence.

The values of τ_ϕ extracted with each of the methods valid beyond the diffusion approximation are very similar. As with the previous sample the Hikami method predicts a much larger phase breaking rate than the other methods. This indicates that the same mechanism (the field sensitivity of $\Delta\sigma_{\rm wl}$) is producing the variation in the value of τ_ϕ extracted from the same data. The values of τ_ϕ extracted using the Dmitriev method agree closely with those of similar *p*-GaAs samples[11] where the method of Wittmann was used.

While the temperature dependence of τ_ϕ is linear there appears to be a nonzero intercept at $T=0$ for each of the densities examined. Proskuryakov *et al.*[11] found a similar result and interpreted their data by adding an offset to the Fermi-liquid prediction of τ_ϕ. This offset is of great interest theoretically as extrapolating the data suggests a finite phase breaking rate at $T=0$. However, caution must be exercised due to the closeness of the data to $\sigma=1$ and the effect that this has on the validity of using weak localization to extract τ_ϕ.

Due to the linearity of the τ_ϕ^{-1} data and because for this data $0.06 < k_B T\tau/\hbar < 0.58$ we compare the T402/5 data to Fermi-liquid theory in the $k_B T\tau/\hbar \ll 1$ limit. For the higher densities, presented in Figs. 6(b) and 6(c), there is good quantitative agreement between the values of the phase breaking rate extracted from the experimental magnetoconductivity using the Dmitirev method and the Fermi-liquid theory prediction of Eq. (16). As the density is decreased further, this agreement becomes rapidly worse and for the lowest density studied, $p = 1.15 \times 10^{10}$ cm^{-2}, Eq. (16) gives an unphysical (negative) value of τ_ϕ for $F_0^\sigma = -0.3$. This is a sign that at these low densities Eq. (16) is outside its range of validity and the system is entering the hopping conduction regime. Nevertheless it is remarkable that Fermi-liquid theory produces a good quantitative agreement with the experimentally extracted values of τ_ϕ for $k_F l$ as low as 1.2.

In summary, Fermi-liquid theory is successful in explaining the phase breaking rate in our high-quality *p*-GaAs samples, until $k_F l$ approaches 1. This indicates that the nature of the hole (or electron) state at these high values of up to $r_s \sim 23$ may be closely related to that at $r_s \sim 12$, which is well explained by Fermi-liquid theory if the correct phase breaking rate is extracted from the experimental data.

V. CONCLUSIONS

We have presented a detailed comparison of five methods of analyzing weak localization data. We demonstrate that the methods of generating $\Delta\sigma_{\rm wl}$ fall into two groups when used to extract the phase breaking rate. The first consists of the Hikami method for diffusive transport and the other of the four methods which are valid beyond the diffusion approximation. We have quantified the range of validity of the Hikami method to be $b \lesssim 0.1$ and $z \lesssim 0.2$. We have shown that the method of Hikami, when applied beyond its range of validity, produces a phase breaking rate approximately three times larger than methods that are valid beyond the diffusion approximation. This largely resolves a puzzling historical discrepancy between Fermi-liquid theory and experiment in which experimentally extracted values of the phase breaking rate were three to five times larger than those predicted by theory.[8,9,12–15]

The four methods valid beyond the diffusion approximation produce very similar values for the phase breaking rate despite differences in the magnitude of the weak localization correction $\Delta\sigma_{\rm wl}$ of up to $\sim$100%. We attribute this to the similarity of the field dependence of the weak localization conductivity correction, $d\Delta\sigma_{\rm wl}/db$, in each of the methods.

For our high-quality *p*-GaAs samples all four methods valid beyond the diffusion approximation predict phase breaking rates with a linear temperature dependence. We also find that Fermi-liquid theory provides a good quantitative prediction of τ_ϕ, even at $r_s \sim 23$. However as $k_F l$ approaches 1 Fermi-liquid theory becomes invalid and the agreement breaks down. Thus Fermi-liquid theory explains the sample properties over its range of validity.

Of the four methods which produce accurate values of τ_ϕ, only the method of Dmitriev[20] (which includes the phase-coherent nonbackscattering mechanism) also produces accurate values of $\Delta\sigma_{\rm wl}$. Failure to use the Dmitriev method may result in errors in $\Delta\sigma_{\rm wl}$ of $\sim$20% at low field and z, and $\sim$200% when either $b \gtrsim 1$ or $z \gtrsim 0.2$ (when either the sample quality or temperature is high). However the method of Dmitriev does not include spin-relaxation effects, so in samples where these are important then the method of Zduniak should be used. At present there seems to be no method in the literature which takes account of both spin-orbit and the phase-coherent nonbackscattering mechanism, and this may be a profitable avenue for further theoretical work.

ACKNOWLEDGMENTS

This work was supported by the Australian Research Council. We thank V.Y. Katchorovskii and A.P. Dmitriev for several useful discussions.

APPENDIX A

Typographical errors in several references discussed in this paper [in addition to Eq. (13)] are corrected below. Note

that the equations below appear exactly as they should in the original works and do not follow the notation adopted in this paper.

Equation (A4) from Kawabata[17] should read[8]

$$Q_0 = \sqrt{\frac{\pi}{2}} \exp\frac{s^2}{2} \mathrm{erfc}\left(\frac{s}{\sqrt{2}}\right). \tag{A1}$$

In Wittmann and Schmid[18] equations (22), (28), (29) and (31) (Ref. 11) should be replaced by the following:

$$\xi^{-1} e^{-\xi} = \int_0^\infty dt\, t(1+t^2)^{-1/2} J_0(\xi t), \tag{A2}$$

$$C_m(b) = \frac{1}{m}\left\{\frac{2}{b}[C_{m-1}(b) - (-2)^{m-1}] - \sum_{k=0}^{m-1} (-2)^{m-1-k} C_k(b)\right\}, \tag{A3}$$

$$\psi_n(b) = [1 + (2n+1)b]^{-1/2} \times \sum_{k=0}^{\infty} M_n^k \frac{(-1)^k}{2^k k!}\left(\frac{1}{2}\right)_n \left[\frac{b}{1+(2n+1)b}\right]^k, \tag{A4}$$

$$\Delta^2 g(B) = \frac{-g_0}{(1+\gamma)^2}\left[\sum_{n=0}^{N} \frac{b\psi_n^3(b)}{1+\gamma-\psi_n(b)} - \ln\frac{1+\gamma}{\gamma}\right]. \tag{A5}$$

APPENDIX B

This appendix describes the solution of Eqs. (5) and (13) (i.e., the method of finding P_n and P_n^m). This allows calculation of the weak localization correction to the conductivity $\Delta\sigma_{\mathrm{wl}}$ for the Kawabata, Wittmann, Zduniak, and Dmitriev methods [it is not necessary for the Hikami method as Eq. (4) is analytic] using Eq. (15) with F_A and F_B defined appropriately for the method as described in Sec. II.

Several techniques exist in the literature to calculate P_n. Kawabata[17] gave a recursive technique, Wittmann[18] proposed both a recursive technique, and one based around a series expansion of Eq. (5). Zduniak[19] and Dmitirev[20] used numerical integration of Eq. (5) [and Eq. (13) for Dmitriev].

Each of these techniques for calculating P_n has a different range of validity (in a two-dimensional b-n space). From the various techniques we must mix and match different techniques to calculate P_n over the full range of n necessary. The recipe given here is valid for the range $0.01 < b < 1000$ and $0.001 < z < 0.5$. These ranges are sufficient to analyze any currently available experimental device.

As well as its intrinsic validity each technique also has an associated computational complexity. If an iterative fitting approach is taken to a large body of data the computational burden imposes an additional constraint on the applicable range of each technique. In particular, we note that accurate numeric integration becomes computationally expensive for the iterative solution of a large volume of data at quite modest values of n ($\sim$20 on a desktop PC). This rules out numerical integration as a practical technique for fitting large volumes of experimental data. Extreme care must also be taken in numerical integration at large values of n due to the rapid oscillation of $P_n(b)$. Problems may also arise from taking the exponent of $s^2/2$ at low b, however, these can be resolved by expanding erfc $(s/\sqrt{2})$ as a series and canceling the exponent terms.

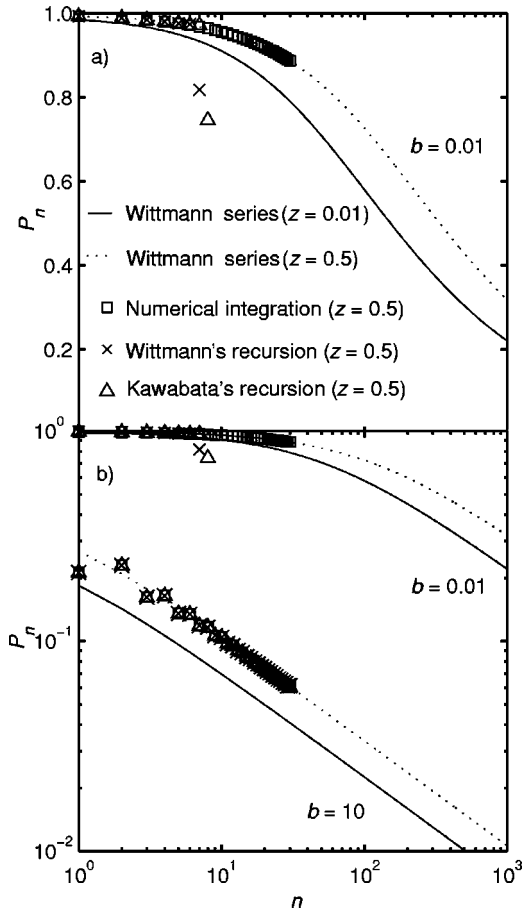

FIG. 8. (a) P_n generated by the techniques described in text for $z=0.01$ and $z=0.5$ with $b=0.01$, (b) P_n generated for $z=0.01$ and $z=0.5$ at $b=0.01$ or 10 for the two groups of curves as indicated.

Figure 8(a) presents P_n for the different calculation techniques at the extremes of the range of z with low b. In order to study the validity of the various techniques of finding P_n over the range of b and z, we replot the data of Fig. 8(a) on a logarithmic scale in Fig. 8(b) and add the equivalent plots for large b.

The two recursion methods are only stable at relatively low n. This can be seen in Fig. 8(a) where the recursion technique solutions both deviate abruptly from the series truncation and numerical integration solutions at $n \sim 7$. In contrast Fig. 8(b) shows that they are stable to larger $n \sim 250$ at high b. This behavior is due to their sensitive dependence on the initial value and the inverse exponential dependence of the first term [given by Eq. (A1)] on b. For large n we find $P_n \propto n^{-1/2}$ with a transition at lower n when b is large. This may be understood by examining Eq. (A4) and noting that $\psi_n \propto P_n$ and that the sum tends to unity at large n. This allows P_n to be efficiently found by truncating the series expansion at large n and b.

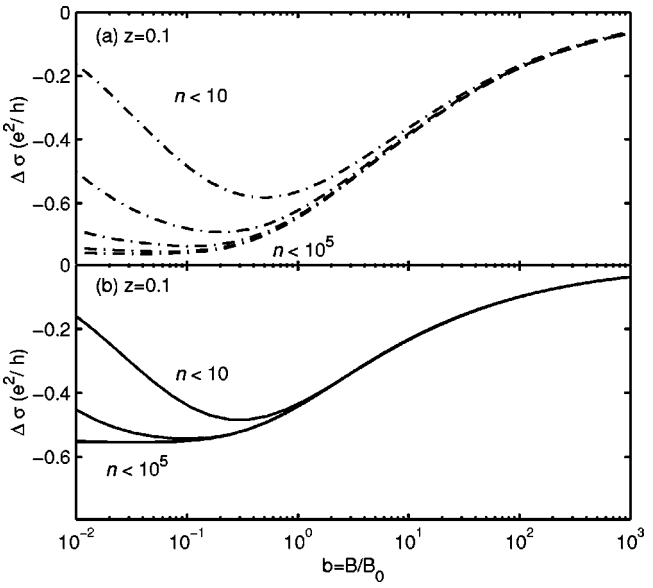

FIG. 9. $\Delta\sigma_{\mathrm{wl}}$ generated with a truncated series expansion for (a) Zduniak and (b) Dmitriev methods. Each expansion is truncated at $n=10$, 10^2, 10^3, 10^4, or 10^5 terms as indicated.

At high b the numerical integration and recursion relation solution oscillate at low n, but the series expansion does not replicate this behavior. Therefore the series expansion should be avoided at low n and high b.

No one technique is valid over the whole range of b, z, and n. It would be awkward to specify the ranges of validity of the various techniques over a space of three variables, so we considered the possibility of ignoring either b or z in the choice of technique used to calculate P_n. Figure 8(b) demonstrates the sensitivity of P_n to variation in b and z over the range of b and z that we will need to analyze our experimental data. P_n varies dramatically in form as b is changed from its minimum through to its maximum with z fixed but only modestly as z is swept from its minimum to maximum with b fixed. That is, the value of $P_n(b,z)$ is sensitive to b but insensitive to z. Therefore for simplicity the value of z is ignored when choosing the technique used to generate P_n, so that the technique used is dependent only on b and n.

P_n has an appreciable value up to large values of n at low b. This means that the series of Eq. (6) must be summed to large n for an accurate estimate of $\Delta\sigma_{\mathrm{wl}}$. Figure 9 shows the effect of truncation of the series at too low a n by plotting the predictions of the Zduniak and Dmitriev methods (Hikami and Kawabata do not suffer this problem) for n up to 10, 10^2, 10^3, 10^4, or 10^5. The problem can be seen to be far more severe for Zduniak (and Wittmann) than for Dmitriev as for Dmitriev the large n contributions for the backscattering and nonbackscattering mechanisms cancel out to some extent (see below).

It can be seen that terms up to $n=10^5$ are necessary to produce accurate results down to $b\sim 0.01$ in the Zduniak (and Wittmann) method and for $z>0.1$ terms up to $n=\infty$ must be included. The effect of truncating at too low a n closely resembles that of spin-relaxation-induced antilocalization,[19] so it is important to select a sufficiently high n to avoid confusing the two.

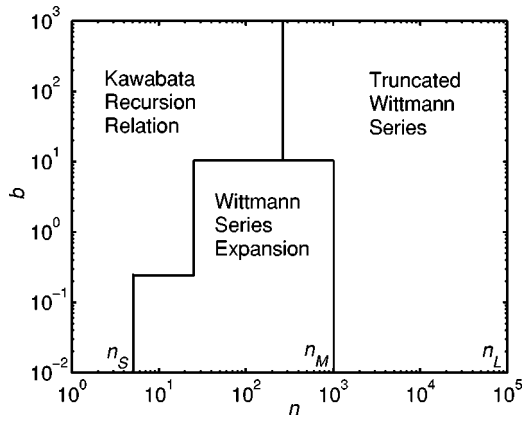

FIG. 10. Diagram of computation method used to calculate P_n. Beyond $n=10^5$ P_n is calculated using Eq. (B2) for all b. The small, medium, and large boundaries n_S, n_M, and n_L are marked at $b=0.01$.

We can now specify ranges in b and n over which the different techniques must be used. To account for the various ranges of validity of the different techniques four regions are specified in n with boundaries n_S, n_M, and n_L (for small, medium, and large). As pictured in Fig. 10, $n_S=n_M=250$ for $b>10$ and $n_L=10^5$ for all b. At $n<n_S$ the recursion relation due to Kawabata is used, as this was found to be slightly more numerically stable than the Wittmann recursion relation. As b increases the range of stability of the recursion relations increases. Therefore the recursion relations, which are fast and accurate until they become unstable, are used over a greater range of n at high b.

For $n_S>n>n_M$ the series expansion method of Wittmann and Schmid is used. This produces accurate and efficient results at intermediate n but fails at high b and low n where it does not reproduce the oscillating behavior of the solution, see Fig. 8(b).

At large n we see that P_n has an inverse square-root dependence on n, demonstrated by the linear regions of Fig. 8(b). Therefore we can improve the speed of our fitting by truncating Wittmann's series expansion [the actual equation that we truncate is Eq. (A4) as the summation term in it tends to 1 at large n and $\psi_n=(1+z)P_n$]. For $n_M>n>n_L$ truncation of Wittmann's series expansion (note the different definition of b by Wittmann and Schmid) gives

$$P_n(b)=\frac{1}{[1+z+(2n+1)b]^{1/2}}. \tag{B1}$$

Beyond $n=n_L$ the assumption $P_n\ll 1$ enables us to produce an analytic sum to infinity for F_A from the power-law dependence. For $n\gg 1$ and $P_n\ll 1$ this sum may be expressed in terms of Riemann series. Common numerical tools[24] allow the contribution for $n>n_L$ to be found, in the case $n_L=10^5$,

$$F_A(n>10^5)=\left(\frac{1}{2b}\right)^{3/2}\left(6.329\times 10^{-3}+\frac{1}{\sqrt{2b}}10^{-5}\right), \tag{B2}$$

up to terms in $1/n^2$ in Eq. (12).

So far we have devoted considerable effort to the solution of Eq. (5). Rather than repeat this entire process for Eq. (13) we express P_n^m in terms of P_n using the identities[24,42]

$$L_n^1(t^2) = -\frac{d}{d(t^2)}L_{n+1}(t^2) \tag{B3}$$

and

$$L_n^{\alpha-1}(t^2) = L_n^\alpha(t^2) - L_{n-1}^\alpha(t^2). \tag{B4}$$

From the latter we find

$$L_n^1(t^2) = \sum_{i=0}^{n} L_i^0(t^2). \tag{B5}$$

The integral of Eq. (13) may be solved by using Eq. (B3) and integrating by parts to give, for $m=1$,

$$2\int_0^\infty dt\ t\ L_n^1(t^2)e^{-st-t^2/2} = 1-(1+z)P_{n+1} - \int_0^\infty dt\ t[L_{n+1}^1(t^2) - L_n^1(t^2)]e^{-st-t^2/2}. \tag{B6}$$

Use of Eq. (B5) then enables us to rewrite this as the recursion relation

$$\int_0^\infty dt\ t\ L_n^1(t^2)e^{-st-t^2/2} = 1-(1+z)P_n - \int_0^\infty dt\ t\ L_{n-1}^1(t^2)e^{-st-t^2/2} \tag{B7}$$

with the zeroth term given by

$$\int_0^\infty dt\ t\ L_0^1(t^2)e^{-st-t^2/2} = 1 - se^{s^2/2}\sqrt{\frac{\pi}{2}}\mathrm{erfc}\left(\frac{s}{\sqrt{2}}\right), \tag{B8}$$

which finally gives

$$P_n^m = \frac{s}{\sqrt{n+(1-m)/2}}\left(1-(1+z)P_{n-(1+m)/2} - \frac{\sqrt{n-1+(1-m)/2}}{s}P_{n-1}^m\right). \tag{B9}$$

Equation (13) can now be computed from the known values of P_n up to $n=10^5$. However P_n^m decreases slowly with increasing n and terms beyond $n=10^5$ cannot be safely neglected if z is large [if z is small Eqs. (B2) and (B11) cancel to leading order]. Therefore above $n=10^5$ we approximate Eq. (B9) as

$$P_n^m = \frac{s}{2\sqrt{n}}[1-(1+z)P_n]. \tag{B10}$$

Substituting this and Eq. (B1) into Eq. (12) allows us to find the contribution from P_n^m for $n>10^5$ to be

$$F_B(n>10^5) = -\frac{(1+z)^2}{(2b)^{3/2}}\left(6.329\times10^{-3} - \frac{1+2z}{\sqrt{2b}}10^{-5}\right), \tag{B11}$$

including terms up to $1/n^2$ in Eq. (12). This allows $\Delta\sigma_{\mathrm{wl}}(B)$ to be found for all methods.

[1] G. Zala, B. N. Narozhny, and I. L. Aleiner, Phys. Rev. B **64**, 214204 (2001).
[2] V. Karpus, Semicond. Sci. Technol. **5**, 691 (1990).
[3] P. W. Anderson, E. Abrahams, and T. V. Ramakrishnan, Phys. Rev. Lett. **43**, 718 (1979).
[4] P. A. Lee and T. V. Ramakrishnan, Rev. Mod. Phys. **57**, 287 (1985).
[5] M. J. Uren, R. A. Davies, M. Kaveh, and M. Pepper, J. Phys. C **14**, L395 (1981); R. A. Davies and M. Pepper, J. Phys. C **16**, L353 (1983).
[6] D. J. Bishop, R. C. Dynes, and D. C. Tsui, Phys. Rev. B **26**, 773 (1982).
[7] G. Bergman, Phys. Rep. **107**, 1 (1984).
[8] R. Taboryski and P. E. Lindelof, Semicond. Sci. Technol. **5**, 933 (1990).
[9] V. Senz, T. Heinzel, T. Ihn, K. Ensslin, G. Dehlinger, D. Grützmacher, and U. Gennser, Phys. Rev. B **61**, R5082 (2000).
[10] M. Y. Simmons, A. R. Hamilton, M. Pepper, E. H. Linfield, P. D. Rose, and D. A. Ritchie, Phys. Rev. Lett. **84**, 2489 (2000).
[11] Y. Y. Proskuryakov, A. K. Savchenko, S. S. Safonov, M. Pepper, M. Y. Simmons, and D. A. Ritchie, Phys. Rev. Lett. **86**, 4895 (2001).
[12] G. Brunthaler, A. Prinz, G. Bauer, and V. M. Pudalov, Phys. Rev. Lett. **87**, 096802 (2001).
[13] S. Pedersen, C. B. Sørensen, A. Kristensen, P. E. Lindelof, L. E. Golub, and N. S. Averkiev, Phys. Rev. B **60**, 4880 (1999).
[14] M. Y. Simmons, A. R. Hamilton, C. E. Yasin, M. Pepper, E. H. Linfield, D. A. Ritchie, K. W. West, and L. N. Pfeiffer, Phys. Status Solidi B **230**, 81 (2002).
[15] P. T. Coleridge, A. S. Sachrajda, and P. Zawadzki, Phys. Rev. B **65**, 125328 (2002).
[16] S. Hikami, A. I. Larkin, and Y. Nagaoka, Prog. Theor. Phys. **63**, 707 (1980).
[17] A. Kawabata, J. Phys. Soc. Jpn. **53**, 3540 (1984).
[18] H.-P. Wittmann and A. Schmid, J. Low Temp. Phys. **69**, 131 (1987).
[19] A. Zduniak, M. I. Dyakonov, and W. Knap, Phys. Rev. B **56**, 1996 (1997).
[20] A. P. Dmitriev, V. Yu. Kachorovskii, and I. V. Gornyi, Phys. Rev. B **56**, 9910 (1997).
[21] W. Knap, C. Skierbiszewski, A. Zduniak, E. Litwin-Staszewska, D. Bertho, F. Kobbi, J. L. Robert, G. E. Pikus, F. G. Pikus, S. V. Iordanskii, V. Mosser, K. Zekentes, and Yu. B. Lyanda-Geller, Phys. Rev. B **53**, 3912 (1996).

[22] A. V. Germaneko, G. M Minkov, O. E. Rut, and A. A. Sherstobitov, 15th International Conference on High Magnetic Fields in Semiconductor Physics, Oxford, UK (unpublished).
[23] S. Hershfield and V. Ambegaokar, Phys. Rev. B **34**, 2147 (1986).
[24] G. Arfken, *Mathematical Methods for Physicists* (Academic Press, New York, 1985).
[25] V. Y. Kachorovskii and A. P. Dmitriev (private communication).
[26] M. Y. Simmons, A. R. Hamilton, M. Pepper, E. H. Linfield, P. D. Rose, D. A. Ritchie, A. K. Savchenko, and T .G. Griffiths, Phys. Rev. Lett. **80**, 1292 (1998).
[27] A. R. Hamilton, M. Y. Simmons, M. Pepper, E. H. Linfield, and D. A. Ritchie, Phys. Rev. Lett. **87**, 126802 (2001).
[28] S. J. Papadakis, E. P. De Poortere, H. C. Manoharan, J. B. Yau, M. Shayegan, S. A. Lyon, Phys. Rev. B **65**, 245312 (2002).
[29] J. J. Hereman, M. B. Santos, K. Hirakawa, and M. Shayegan, J. Appl. Phys. **76**, 1980 (1994).
[30] B. E. Cole, J. M. Chamberlain, M. Henini, T. Cheng, W. Batty, A. Wittlin, J. A. A. J. Perenboom, A. Ardavan, A. Polisski, and J. Singleton, Phys. Rev. B **55**, 2503 (1997).
[31] H. L. Störmer, Z. Schlesinger, A. Chang, D. C. Tsui, A. C. Gossard, and W. Wiegmann, Phys. Rev. Lett. **51**, 126 (1983).
[32] M. Kubisa, L. Bryja, K. Ryczko, J. Misiewicz, C. Bardot, M. Potemski, G. Ortner, M. Bayer, A. Forchel, and C. B. Sørensen, Phys. Rev. B **67**, 035305 (2003).
[33] W. Poirier, D. Mailly, and M. Sanquer, Phys. Rev. B **57**, 3710 (1998).
[34] The residual of each fitted point is the difference between the experimental data and the fit value. A perfectly fitted function would differ only due to statistical noise and so the residuals would be positive and negative at random, i.e., completely uncorrelated.
[35] G. M. Minkov, A. V. Germanenko, V. A. Larionova, S. A. Negashev, and I. V. Gornyi, Phys. Rev. B **61**, 13 164 (2000).
[36] O. Prus, M. Reznikov, U. Sivan, and V. Pudalov, Phys. Rev. Lett. **88**, 016801 (2002).
[37] M. Rahimi, S. Anissimova, M. R. Sakr, S. V. Kravchenko, and T. M. Klapwijk, Phys. Rev. Lett. **91**, 116402 (2003).
[38] B. N. Narozhny, G. Zala, and I. L. Aleiner, Phys. Rev. B **65**, 180202(R) (2002).
[39] H. Fukuyama and E. Abrahams, Phys. Rev. B **27**, 5976 (1983).
[40] B. L. Altshuler and A. G. Aronov, in *Electron-Electron Interactions in Disordered Systems*, edited by A. L. Efros and M. Pollack (North-Holland, Amsterdam, 1985).
[41] Y. Y. Proskuryakov *et al.*, Phys. Rev. Lett. **89**, 076406 (2002).
[42] A. Erdélyi, *Higher Transcendental Function* (McGraw-Hill, New York, 1953), Vol. 2.